Long-term measurements of aerosol composition at rural background sites in France: sources, seasonality and mass closure of PM2.5.

Anna Font, Joel F. de Brito, Véronique Riffault, Sébastien Conil, Jean-Luc Jaffrezo, Aude Bourin

Atmospheric Environment 334 (2024) 120724

Contents lists available at ScienceDirect

Atmospheric Environment

journal homepage: www.elsevier.com/locate/atmosenv

Long-term measurements of aerosol composition at rural background sites in France: Sources, seasonality and mass closure of $PM_{2.5}$

Anna Font [a,*], Joel F. de Brito [a], Véronique Riffault [a], Sébastien Conil [b], Jean-Luc Jaffrezo [c], Aude Bourin [a]

[a] IMT Nord Europe, Europe, Institut Mines-Télécom, Univ. Lille, Centre for Education, Research and Innovation in Energy Environnement (CERI EE), 59000, Lille, France
[b] ANDRA DISTEC/EES Observatoire Pérenne de l'Environnement, F-55290, Bure, France
[c] Institut des Géosciences de l'Environnement (IGE) CNRS, UGA, IRD, Grenoble INP, 38058, Grenoble, CEDEX, France

HIGHLIGHTS

- $PM_{2.5}$ exceeded health guidelines at rural background sites in France in 2012–2021.
- OM accounted for the largest $PM_{2.5}$ component followed by secondary inorganics.
- Biomass burning is the main primary source of $PM_{2.5}$: 17–27% of total $PM_{2.5}$
- Mitigation of nitrate and ammonium precursors required to reduce $PM_{2.5}$ levels.

GRAPHICAL ABSTRACT

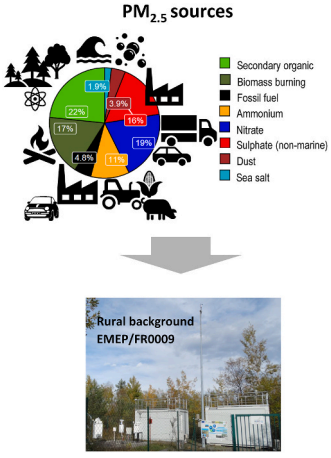

ARTICLE INFO

Keywords:
Fine particles
Mass closure
Organic matter
Secondary inorganic aerosol
Biomass burning

ABSTRACT

Fine particulate matter ($PM_{2.5}$) was monitored at five rural background locations in France from 2012 to 2021. Annual $PM_{2.5}$ ranged from 5 to 15 μg m^{-3}, all sites repeatedly exceeding the 2021 annual World Health Organization guideline. Chemical speciation including organic and elemental carbon (OC, EC), secondary inorganic aerosols (SIA: NO_3^-, SO_4^{2-}, NH_4^+) and other major water-soluble ions (Cl^-, Na^+, Mg^{2+}, Ca^{2+}, K^+) were monitored on 24-h filters covering 14% of the year. A source apportionment of OM was undertaken based on fine potassium and using representative ratios for domestic biomass burning (BB) and fossil fuel (FF) emissions. The latter dominated the EC fraction (55–60%) while BB was the main primary source of OM (27–54%). The average mass balance of $PM_{2.5}$ at the French rural background atmospheric sites was: secondary organic aerosol (18–35%), BB (17–27%), non-sea-salt sulphate (12–17%), nitrate (6–22%), ammonium (7–11%), FF (4–6%), mineral dust (3–9%) and sea salt (1–2%). Secondary aerosols were the main component of $PM_{2.5}$ through all seasons, with SIA dominating in spring episodes. The contribution of OM to $PM_{2.5}$ was larger at the southern sites whereas the

* Corresponding author.
E-mail address: anna.font@imt-nord-europe.fr (A. Font).

https://doi.org/10.1016/j.atmosenv.2024.120724
Received 1 March 2024; Received in revised form 23 July 2024; Accepted 26 July 2024
Available online 27 July 2024

contribution of SIA was larger at the northern sites. The mean OC/EC ratio and the good correlations between OC, EC, and fine potassium suggested that BB was the main primary source contributing to carbonaceous aerosols, 27–54% to total OM depending on the site; and also, to $PM_{2.5}$ (17–27%). Stronger regulations of OM sources including BB, nitrate from combustion, and ammonium from agricultural sources are needed to reduce $PM_{2.5}$ at rural background sites on an annual and episodic basis, respectively.

1. Introduction

Suspended particulate matter (PM) in the atmosphere is well known to have an impact on climate, environment and human health (IPCC, 2021). The aerosol composition is highly variable in space and time and depends upon (i) the relative contributions from sources including natural (e.g., sea salt, mineral dust, biogenic) and/or anthropogenic (agriculture, combustion, traffic, etc.) emissions; (ii) the reactivity in the atmosphere (e.g., gas-to-particle transformations); as well as (iii) the meteorological conditions and regional or long–range transport (Seinfeld and Pandis, 2006). Routine measurements of the gravimetric mass of fine particles (particles with a mean aerodynamic diameter <2.5 μm or $PM_{2.5}$) and their chemical components are important to investigate the temporal and spatial variabilities of concentrations; and to investigate the sources contributing to aerosol levels, essential for climate change and health studies. The revision of the EU directive on ambient air quality and cleaner air for Europe (EC, 2022) proposes the reduction of exposure to $PM_{2.5}$ levels by bringing their limit values closer to World Health Organization (WHO) guidelines. The latter were revised in autumn 2021 and lowered the $PM_{2.5}$ annual guideline from 10 μg m^{-3} to 5 μg m^{-3}; and the daily guideline from 25 μg m^{-3} to 15 μg m^{-3}. Improving the knowledge of the major sources contributing to $PM_{2.5}$ is therefore critical to design effective emission reduction and mitigation strategies.

Background areas are located away from the direct influence of urban and industrial emissions but remain influenced by emissions at the regional scale. Studies of aerosol composition at remote sites in Europe were previously reported by Pio et al. (2007) where the aerosol composition at five remote locations across Europe was measured over two years, thus providing their spatial variability and the mass partitioning. Conversely, Putaud et al. (2004, 2010) summarized the aerosol composition across Europe at rural, urban and roadside sites, and Alastuey et al. (2016) examined the different sources contributing to PM_{10} mass at background sites as part of the European Monitoring and Evaluation Programme (EMEP). In France, multi-year mass balance studies of PM include the remote site of Verneuil in 2011–2014 (He et al., 2018) and at OPE for a nine–year period (Borlaza et al., 2022).

Carbonaceous particles are a major component of fine aerosols (Christiansen et al., 2020; Golly et al., 2019; Querol et al., 2013; Yttri et al., 2009, 2021). Organic carbon (OC) can be emitted directly by primary sources including fossil fuel, biomass burning and biological plants and debris, or formed secondarily from gaseous precursors. Elemental carbon (EC) is emitted from primary sources including combustion processes such as transport, industries or biomass burning (BB). Given that carbonaceous matter represents a major component of PM in France (Weber et al., 2019), the apportionment of both EC and OC is a necessary step towards reducing $PM_{2.5}$ levels.

Here we report a decade of $PM_{2.5}$ mass and chemical speciation at five rural background sites in France belonging to the MERA network (acronym in French: *Mesure et Evaluation en zone Rurale de la pollution Atmosphérique à longue distance*), and the OPE site (*Observatoire Pérenne de l'Environnement*) (Golly et al., 2019), all contributing to EMEP. The seasonal and spatial variability of aerosol composition and sources are discussed. These results evaluate the variability of $PM_{2.5}$ background in French rural areas, contribute to the long–term studies of aerosol composition for climate studies and emission evaluation, and help identifying sources that should be prioritized towards improving the air quality and human health in light of the forthcoming new EU directive (EU, 2022).

2. Methods

2.1. Description of the sites

Five rural background sites in France monitored $PM_{2.5}$ mass concentrations and chemical composition for the period 2012–2021 (Fig. 1). Four of them (PEY, REV, SND and VER) belong to the MERA observatory and integrated in the French air quality network, managed locally by the regional Approved Air Quality Monitoring Associations (AASQAs in French) and nationally by IMT Nord Europe. The OPE station is managed by ANDRA (the French national radioactive waste management agency) with the support of one of the AASQA (Atmo Grand Est), and chemical analyses are performed at the Institute of Geosciences and the Environment (Borlaza et al., 2022; Golly et al., 2019). A short description of the monitoring sites can be found in the Supplementary Information (SI, section 1).

2.2. Sample collection and measurement techniques

Twenty-four-hour filter samples, starting at 9 a.m. GMT, were sampled for chemical composition of $PM_{2.5}$ every sixth day, covering ~14% of the year in response to the EU Directive 2008/50/CE. Quartz filters (Pallflex Tissuquartz 2500 QAT-UP, 150 mm in diameter) were preconditioned (pre-fired for 24 h at 773 K) and later exposed to ambient air using High-Volume Samplers (HVS Digitel DAH-80) equipped with a $PM_{2.5}$ inlet and sampling at 30 m^3 h^{-1}. The samplers were placed in temperature-controlled stations (20–23 °C) to limit the loss of semi-volatile species. A total of 2176 filters were analysed over the study period for organic and elemental carbon (OC, EC) and inorganic ions (Ca^{2+}, K^+, Mg^{2+}, Na^+, NH_4^+; and Cl^-, NO_3^-, SO_4^{2-}). Details about the chemical analysis can be found elsewhere (Font et al., submitted) and a summary is in S2 of the SI. Besides, levoglucosan was measured in 2012–2021 at OPE (Borlaza et al., 2022); 2012–2015 at PEY and REV; and 2014–2015 at SND and VER.

Collocated in-situ observations of non-refractory PM_1 chemical composition were conducted at REV in the summer of 2012 (24 Jun–14 Jul). An aerosol mass spectrometer (AMS, Aerodyne Research Inc., USA; 5-min resolution) yielded OM, sulphate, nitrate, and ammonium concentrations. Positive Matrix Factorization (PMF) of the organic spectra was undertaken and three factors of organic aerosol (OA) were identified: hydrogen-like OA associated with traffic emissions; biomass burning OA; and secondary OA (Setyan et al. in prep.).

Hourly $PM_{2.5}$ gravimetric mass was monitored by automatic instruments proved to equivalent to the EU reference methods: Tapered Element Oscillating Microbalance-Filter Dynamics Measurement System (TEOM-FDMS; Thermo R&P; USA); Beta Attenuation Monitor 1020 (BAM, MetOne Instruments Inc; USA); beta gauge MP101MRST (ENVEA; France) or a FIDAS 200 (PALAS; Finland), depending on the site and year. All instruments are accredited to measure PM-equivalent mass concentrations in France (LCSQA, 2013, 2017). Change of instrumentation took place at all sites in the time series. Data collection and validation were conducted by the regional AASQA as part of the French Air Quality Monitoring Program.

2.3. Mass closure calculations

$PM_{2.5}$ mass can be expressed as the addition of its main components:

$$PM_{2.5} = [OM] + [EC] + [SIA] + [sea\ salt] + [dust] + [trace\ elements] + \varepsilon \quad (1)$$

where OM stands for organic matter; SIA for secondary inorganic aerosols which include nitrate, non-sea-salt-sulphate and ammonium. Trace elements include metals and other trace elements such as fine potassium from wood burning. Here, only the non-sea-salt-non-dust potassium (*nss-ndust*-K^+) was included as other trace metals and elements were not routinely analysed at the MERA sites. ε refers to the residual term including the missing mass, errors associated with $PM_{2.5}$ measurements from online instruments and the analytical errors of the chemical analysis. A detailed description of the mass balance calculations is in SI–S3.

OM was estimated from OC from thermo-optical analysis as:

$$[OM] = f_{OM:OC} \times [OC] \quad (2)$$

where $f_{OM:OC}$ is the conversion factor from OC to OM, specific to each monitoring site. Here, site-specific $f_{OM:OC}$ were calculated by relating the unidentified chemical fraction in $PM_{2.5}$ samples to thermo-optical OC concentrations. Details of its calculations are presented elsewhere (Font et al., submitted). Values of $f_{OM:OC}$ used for each site are summarized in Table 1 and ranged from 1.5 to 2.9. The $f_{OM:OC}$ at REV and VER was representative of highly oxidised OM and agreed with the expected $f_{OM:OC}$ of 2.1 for non-urban aerosols (Lim and Turpin, 2002). The $f_{OM:OC}$ at SND and OPE was below the recommended value of 2.1. However, low $f_{OM:OC}$ (1.5–1.6) was previously calculated at a French semi-rural site near Paris (20 km) (Crippa et al., 2013; Petit et al., 2015). PEY had the largest $f_{OM:OC}$ ratio, slightly above the 2.2–2.6 range representative for non-urban sites according to Lim and Turpin (2002), but in agreement with the presence of highly oxidised aerosols.

2.4. Air mass backtrajectories

The HYbrid Single-Particle Lagrangian Integrated Trajectory (HYSPLIT) (Stein et al., 2015) with the global data assimilation system (GDAS) (1° × 1°; 3-h temporal resolution) were used to compute backtrajectories (BTs). For each filter, 72-h BTs were calculated every 3 h at an arrival altitude of 500 m above the ground. Position (latitude, longitude and altitude), rainfall and mixing layer (ML) depth along the BT were extracted hourly.

The identification of potential long-range sources of aerosols was done by means of the Concentration-Weighted Trajectory (CWT) algorithm. CWT maps were computed by the *trajLevel* function from the *openair* R–package (Carslaw and Ropkins, 2012) at a spatial resolution of 0.5° × 0.5°. Trajectory points following a large rain episode (>1 mm) were excluded as in Waked et al. (2018). A minimum of 50 occurrences at a given grid cell was set to be identified as a potential source. To limit the upwind influence area to surface sources BT locations above the ML were excluded. However, as the arrival height was set at 500 m, it was located at times above the ML, particularly in winter nights. Those BT locations within the 150% of the ML height were considered.

3. Results and discussion

3.1. $PM_{2.5}$ concentrations: summary statistics

Annual $PM_{2.5}$ concentrations (measured by the online instruments) ranged from 5 to 15 μg m^{-3} in 2012–2021 at the French rural sites

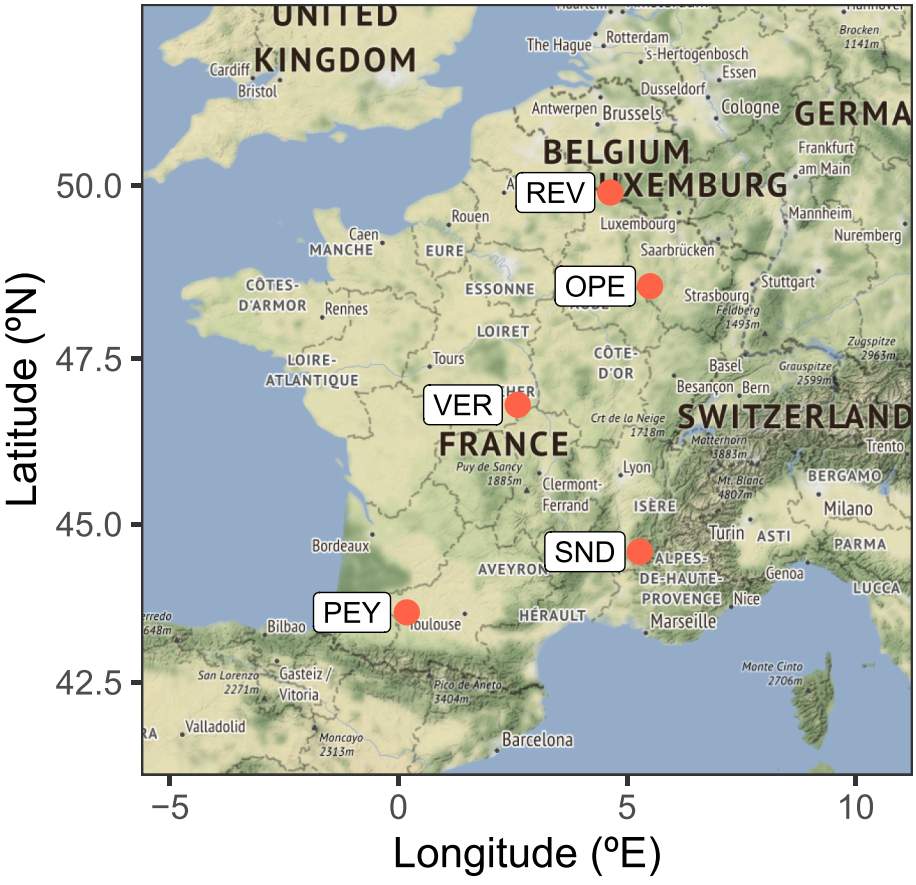

Fig. 1. Selected sites belonging to the rural background network in France.

Table 1
Mean and 95% confidence intervals (in brackets) for $PM_{2.5}$ and its components measured at the French rural sites.

	OPE	PEY	REV	SND	VER
Period	2012–2021	2012–2021	2012–2021	2014–2021	2014–2021
N filters	339	436	485	463	453
$PM_{2.5}$ (μg m^{-3})	11 [9–13]	7.8 [6.8–8.8]	8.8 [7.5–10]	5.5 [4.8–6.2]	7.7 [6.4–8.9]
OC (μg m^{-3})	2.1 [1.7–2.4]	1.7 [1.5–1.9]	1.8 [1.6–2.0]	2.0 [1.8–2.2]	2.0 [1.7–2.2]
EC (μg m^{-3})	0.25 [0.21–0.29]	0.16 [0.14–0.18]	0.20 [0.18–0.22]	0.17 [0.15–0.19]	0.19 [0.16–0.21]
OC/EC	8.9 [7.9–9.9]	13 [11–14]	9.9 [9.0–11]	13 [12–14]	12 [11–13]
NO_3^- (μg m^{-3})	2.4 [1.5–3.2]	0.43 [0.23–0.64]	1.7 [1.2–2.3]	0.39 [0.19–0.60]	0.83 [0.42–1.2]
nss–SO_4^{2-} (μg m^{-3})	1.4 [1.2–1.7]	0.94 [0.79–1.1]	1.4 [1.2–1.6]	0.91 [0.77–1.1]	0.89 [0.72–1.1]
NH_4^+ (μg m^{-3})	1.1 [0.78–1.3]	0.45 [0.35–0.55]	0.96 [0.74–1.2]	0.42 [0.33–0.51]	0.53 [0.38–0.69]
Sea salt (μg/m^{-3})	0.1 [0.06–0.15]	0.12 [0.009–0.15]	0.17 [0.13–0.21]	0.04 [0.03–0.06]	0.13 [0.08–0.18]
Dust (μg/m^{-3})	0.85 [0.60–1.1]	0.21 [0.16–0.27]	0.35 [0.27–0.42]	0.51 [0.40–0.63]	0.30 [0.21–0.40]
K^+ (μg m^{-3})	0.25 [0.21–0.29]	0.05 [0.03–0.06]	0.05 [0.04–0.06]	0.05 [0.04–0.06]	0.04 [0.04–0.05]
nss-ndust-K^+ (μg m^{-3})	0.05 [0.04–0.07]	0.03 [0.02–0.04]	0.04 [0.03–0.05]	0.04 [0.02–0.05]	0.04 [0.03–0.04]
$f_{OM:OC}$	1.8 [1.6–2.0]	2.9 [2.8–3.0]	2.1 [2.0–2.2]	1.5 [1.4–1.6]	2.3 [2.2–2.4]
Quantification of Levoglucosan					
Period	**2012–2021**	**2012–2015**	**2012–2015**	**2014–2015**	**2014–2015**
N filters	339	97	147	123	116
Levoglucosan (ng m^{-3})	93 [68–119]	113 [80–147]	78 [63–93]	65 [50–80]	135 [100–169]

(Table S6). Annual concentrations complied with both the EU limit and target values (25 and 20 μg m^{-3}, respectively); however, most sites and years were above the annual 2021 WHO guideline (5 μg m^{-3}), except 3 years at SND (2019–2021) within its 8-year timeseries; and 1 year at REV (2020) for its 10-year dataset. The number of days with $PM_{2.5}$ exceeding the EU daily limit of 50 μg m^{-3} set for PM_{10} was only 1–3 instances per year. Yet, the daily 2005 WHO guideline (25 μg m^{-3} not be be exceeded more than 3 days per year) was largely exceeded at the northernmost sites (OPE, REV and VER) before 2017; and the daily 2021 WHO guideline (15 μg m^{-3} no more than 4 days per year since 2021) was exceeded at all sites except at SND in 2018 and 2019. Most daily exceedances occurred in March (Fig. S7). More details are available in SI–S5.

3.2. Carbonaceous aerosols: OC and EC

OC was the main component of $PM_{2.5}$ at all sites (except OPE) with mean daily concentrations of 1.7–2.1 μg m^{-3} (Table 1). OC concentrations at the French rural sites were like those in remote and rural areas in Spain (1.2–2.3 μg m^{-3}) (Querol et al., 2013) but lower than mean OC measured at other central European rural background sites (2.85 μg m^{-3}; Mbengue et al., 2018). EC was an order of magnitude lower than OC (0.16–0.26 μg m^{-3}) and concentrations agreed with those at rural sites in Spain (Querol et al., 2013) but again lower than other central European rural background sites (Mbengue et al., 2018). OC and EC correlated at all sites (R^2 = 0.44–0.77) and especially in winter (R^2 = 0.64–0.86) (Fig. S9) suggesting to some extent common sources, particularly in the cold season. Mean OC/EC ratios at the French rural sites in 2012–2021 ranged from 8.9 (OPE) to 13 (SND) (Table 1), consistent with ratios observed at rural and remote sites in Europe (4.9–13.5) (Pio et al., 2011). Ratios at PEY, SND and VER were in the low-to-middle range of those observed at rural sites in Spain (OC/EC = 12–15) (Querol et al., 2013). OC/EC is commonly used to qualitatively assess sources contributing to carbonaceous species: OC/EC < 2 is characteristic of general vehicular emissions (Brito et al., 2013) with OC/EC < 0.5 being ascribed to diesel emissions (Crilley et al., 2015; El Haddad et al., 2009; Zielinska et al., 2004). Ratios of 3–70 are indicative of wood combustion (Ball et al., 2008) with values varying depending on the type of device and combustion conditions: 3.2–10 being typical of stoves; and 10–15 of fireplaces (Calvo et al., 2015). OC/EC at the French rural sites showed a marked monthly variability (Fig. S10) peaking in June–July with summer maxima larger at the southern sites of PEY and SND (ratios around 22), compared to the northern sites (OPE, REV) with ratios of 15. These large summer OC/EC suggest a prevalence of secondary organic aerosol (SOA) resulting mainly from the oxidation of biogenic volatile and/or semi-volatile organic compounds (Golly et al., 2019; Kaskaoutis et al., 2022; Ram et al., 2012). Conversely, ratios were at a minimum in November–December (mean: 5.7–9.7), compatible with values from closed-stove residential heating emissions.

3.3. Levoglucosan and relation to OC, EC and nss-ndust-$K^{\pm}$

Levoglucosan is an anhydrosugar found in woodsmoke in the OC fraction and traditionally used as a BB tracer (Cordell et al., 2014, 2016). Period average concentrations ranged from 135 (VER) to 65 ng m^{-3} (SND) (Table 1) in agreement with levels at rural sites in Austria (150 ng m^{-3}) (Caseiro et al., 2009) and at a rural background site in southern Sweden (56 ng m^{-3}) (Martinsson et al., 2017). Levoglucosan observed a strong seasonal pattern with winter concentrations 16 (REV) to 37 (VER) times larger than in summer. Mean winter concentrations (range from 114 ng m^{-3} at SND to 304 ng m^{-3} at VER) were larger than those at rural sites in south-east England (70–92 ng m^{-3}) (Crilley et al., 2015) and in southern Sweden (86 ng m^{-3}) (Martinsson et al., 2017). Across the different sites, levoglucosan and OC showed low to moderate correlations (R^2 = 0.15–0.52), and stronger in winter (R^2 = 0.40–0.87) (Fig. S11), showing the large influence of BB emissions on OC especially in the cold season.

The OC/levoglucosan ratio is often used to identify episodes of BB with values varying depending on the type of biomass, combustion conditions and atmospheric ageing. An OC/levoglucosan equal to 7.35 was set as representative for stoves and fireplaces in the US (Fine et al., 2002) while (Gelencsér et al., 2007) proposed the range 6–12.5, with the lower bound representative of hard-wood types and the upper for soft-wood fires in stoves and fireplaces (Herich et al., 2014). Winter OC/levoglucosan at the French rural sites ranged from 9.7 (PEY) to 14 (OPE) (Fig. S11B) in agreement with values in Gelencsér et al. (2007) as representative of domestic wood burning. Similarly, levoglucosan and EC correlated moderately at all sites (R^2 = 0.43–0.57) but larger in winter (R^2 = 0.50–0.70) (Fig. S12) corroborating the expected influence of BB emissions in winter EC.

Levoglucosan was not consistently measured across the dataset. Despite its multiple sources, fine potassium (K^+) is also commonly used as a proxy for BB emissions (Allen and Miguel, 1995; Andreae, 1983; Harrison et al., 2012; Hsu et al., 2009). As levoglucosan, *nss-ndust*-K^+ showed larger concentrations from November to March (Fig. S13A) in agreement with the seasonality of domestic wood burning emissions. Correlations between *nss-ndust*-K^+ and levoglucosan were strong at OPE and VER in winter (R^2 > 0.56) whereas low at PEY, SND and REV (Fig. S13B). Removing those filters with K^+ below the LoD and those instances with very large K^+ not associated with levoglucosan improved the correlation at PEY and REV (Fig. S13B). A possible explanation of the mismatch between levoglucosan and *nss-ndust*-K^+ at SND could be the

oxidation of levoglucosan (Hoffmann et al., 2010), which is considered a good tracer for BB only for freshly emitted particles close to the source. Levoglucosan degrades by oxidation with the hydroxyl radical (Hennigan et al., 2010), which is affected by high relative humidity (Hoffmann et al., 2010) and ageing during long-range transport (Lai et al., 2014). The levoglucosan lifetime in the atmosphere ranges from less than a day (in summer) to up to 26 days (Bhattarai et al., 2019). Conversely, potassium is not known to chemically degrade in the atmosphere (Li et al., 2021). Another possible explanation is the contamination of filters by insects that might lead to spikes in K^+ and not in levoglucosan.

3.4. Apportionment of carbonaceous aerosols

OM was calculated from OC concentrations by means of Eq. (2). Both OM and EC were apportioned by the different sources. The contribution of BB to both OM (OM_{bb}) and EC (EC_{bb}) was estimated using *nss-ndust*-K^+ as a tracer. A representative OM/*nss-ndust*-K^+ = 38.2 for biofuel was used, from the average OC and K concentrations reported in Andreae (2019) and converting OC to OM with $f_{OM:OC}$ = 1.6. This ratio agreed with observed winter ratios at the French rural sites (Fig. S14B).

$$OM_{bb} = 38.2 \times [nss\text{-}ndust\text{-}K^+] \quad (3)$$

Conversely, a representative EC/K = 6.2 ± 3.3 for biofuel was reported in Andreae (2019) but this ratio is larger than those at the sites here (range: 1.7–2.7) (Fig. S15A). Alternatively, the winter 20% lowest EC/*nss-ndust*-K^+ were consistent among all sites (range: 1.6–2.7) and the median value was thus used (EC/*nss-ndust*-K^+ = 2.1) as representative for BB emissions for this dataset. EC_{bb} and EC_{ff} were then calculated as:

$$EC_{bb} = 2.1 \times [nss\text{-}ndust\text{-}K^+] \quad (4)$$

$$EC_{ff} = EC - EC_{bb} \quad (5)$$

OM could be split into different components:

$$OM = OM_{ff} + OM_{bb} + OM_{soa} + OM_{PBOA} \quad (6)$$

where OM_{ff} is the OM from FF combustion; OM_{soa} is the fraction associated with SOA, and OM_{PBOA} stands for primary biogenic organic aerosols including spores, pollen, etc. OM_{PBOA} is supposed to be negligible in the fine fraction (Golly et al., 2019; Samaké et al., 2019) and not considered here. OM_{ff} was calculated from EC_{ff} using a representative ratio. The ratio reported at the French remote site of Puy de Dôme between the hydrogen–like organic aerosol from positive matrix factorization (PMF) of OM spectra and black carbon was 2.4 (Chen et al., 2022). This ratio was larger than the OM/EC = 0.58 reported from tunnel measurements in France (El Haddad et al., 2009) but close to the ratio from the industry/traffic profile at a remote site in Norway (2.24) (Yttri et al., 2021) and slightly lower than the ratio from the traffic factor at OPE (3.8) (Borlaza et al., 2022). The ratio of 2.4 was thus taken as

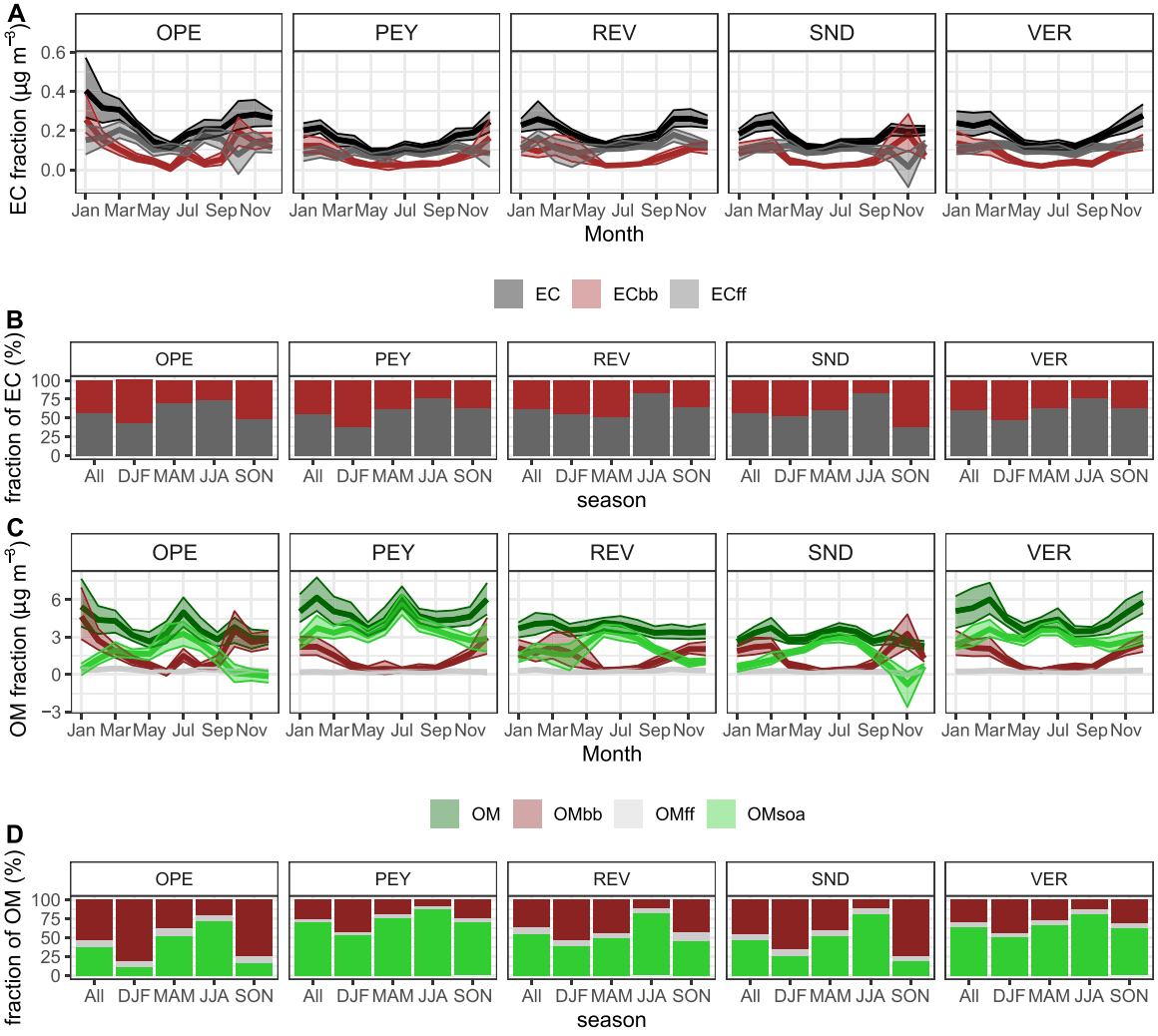

Fig. 2. Source apportionment of elemental carbon (EC) and organic aerosols (OM): monthly variation (A; B); contribution to total EC and OM on a seasonal basis (C, D).

representative of rural sites in France.

OM_{ff} and OM_{SOA} were then calculated as:

$$OM_{ff} = 2.4 \times EC_{ff} \quad (7)$$

$$OM_{SOA} = OM - OM_{bb} - OM_{ff} \quad (8)$$

EC was dominated by FF at all sites, with a contribution of 55–60% to total EC considering the whole period. Concentrations of EC_{bb} were in the range of 0.07–0.11 μg m^{-3} (38–45% of total EC) and showed the expected seasonality associated with BB emissions (Fig. 2A and B). At OPE, EC_{ff} and EC_{bb} represented 56% and 45% of total EC, respectively, close to the allocation of EC from PMF results on PM_{10} at the same site: 42% (traffic factor) and 25% (BB), with the rest of the EC associated to the aged sea salt and the methanesulfonic acid-rich factors (Borlaza et al., 2022). Concentrations of OM_{bb} were 1.3–2.0 μg m^{-3}, representing 27–54% of total OM depending on the site. Winter OM_{bb} ranged from 1.8 μg m^{-3} at SND (65% of OM), to 3.4 μg m^{-3} at OPE (81% of OM). There were some residual summer OM_{bb} concentrations, ranging from 0.39 μg m^{-3} at SND (11% of total OM for the period); to 0.85 μg m^{-3} at OPE (21% of OM) (Fig. 2D). Mean concentrations of OM_{ff} ranged from 0.21 to 0.33 μg m^{-3} (4–9% of OM) with little seasonal variability (Fig. 2C and D). The contribution of OM_{SOA} to total OM was 38–69%, with a mean concentration for the whole period ranging from 1.4 to 3.4 μg m^{-3}. OM_{SOA} showed a marked seasonal variability, with larger concentrations in summer (range: 2.9–4.4 μg m^{-3}; 72–87%) than in winter (0.5–3.1 μg m^{-3}; 11–53%) (Fig. 2C and D). The method for these estimations indeed shows some limitations, with an estimated negative contribution for OM_{SOA} calculated in winter at SND, associated with larger concentrations of OM_{bb} than total OM (Fig. 2C).

OM_{SOA} showed moderate to large correlations to daily maximum O_3 at all sites in summer (range in R: 0.6–0.8, statistically significant at $p < 0.001$) but not in winter, in agreement with the oxidation of biogenic VOCs in summer (Xu et al., 2015). Also in summer, OM_{SOA} moderately correlated to both NH_4^+ and *nss*-SO_4^{2-} (range in R: 0.3–0.5, $p < 0.001$). For the other seasons, correlations between OM_{SOA} and SIA varied depending on the site. REV and VER observed large correlations in winter (R = 0.6–0.7, $p < 0.001$); however, REV observed no correlation in spring (Fig. S16). SOA and SIA are only expected to correlate when (i) the air originates from upwind sources emitting precursors of both SIA and SOA, and (ii) the processes favouring their formation are met locally or during transport, such as enhanced photochemistry. Both EC_{bb} and OM_{bb} showed strong correlations to winter NO_2 (range in R: 0.7–0.9, $p < 0.001$) at all sites except SND where the correlation was weaker (R = 0.3) but statistically significant ($p < 0.001$). Conversely, correlations were weaker in summer, which is an indication that biomass burning was the main source of combustion in winter at the regional background sites. It was in summer when EC_{ff} and OM_{ff} showed the largest correlations to NO_2 (Fig. S16).

3.5. Comparison of methods for carbonaceous source apportionment

The source apportionment of OM from the filter tracer method was compared to that from the PMF on the spectra of the AMS (AMS-PMF) in summer 2012 at REV. Only two days were available for comparison and the temporal trend of OM sources was the same as calculated by the two methods (Fig. 3A). SOA represented 84 and 75% according to AMS-PMF and filter tracer methods, respectively, albeit with significant differences in total OM (4.2 μg m^{-3} for the former and 2.4 μg m^{-3} for the latter) due to the conversion factor to calculate OM from OC thermo-optical filter measurements (Fig. 3B). The FF contribution was 16% and 10% of total OM as predicted by the AMS-PMF and the filter methods, respectively. Finally, the filter tracer method identified a non-negligible contribution of BB (0.36 μg m^{-3}; 15% of total OM), not identified by the AMS, indicative of the uncertainty in the methods or different tracers used. While the filter method is based on *nss-ndust*-K^+, the AMS source apportionment is based on levoglucosan having a significantly shorter lifetime due to its degradation with warmer and more humid conditions as expected in summer (Hoffmann et al., 2010) and exposure to OH radicals (Hennigan et al., 2010). However, the use of potassium as a tracer of BB emissions is not free from uncertainties: multiple sources exist and the isolation of dust and sea salt influence based on fixed elemental ratios might not be accurate in all conditions. Overall, the filter method predicted OM_{ff} and OM_{SOA} concentrations 64% and 48% lower than the AMS-PMF, respectively.

Other comparisons are available at OPE where PMF applied to PM_{10} chemical composition showed that BB contributed to 9% of PM_{10} in 2012–2020, with a mean concentration of 2.0 μg m^{-3} (Borlaza et al., 2022). Estimations for the same site based on the tracer method applied to $PM_{2.5}$ in 2012–2021 agreed, with an average concentration of 2.2 μg m^{-3} (considering BB = OM_{bb} + EC_{bb} + *nss-ndust*-K^+). It is expected that those values are comparable despite the different size ranges, given that BB emissions are mostly found in the fine mode (Jaffrezo et al., 2005; Reid et al., 2005). Traffic emissions, the only FF source identified at the site, represented ~1 μg m^{-3} of PM_{10} (Borlaza et al., 2022) and about half of it to $PM_{2.5}$ (this study). Discrepancies here might be associated with the PM fraction used, with traffic resuspension and non-exhaust emissions mostly found in the coarse fraction (thus in PM_{10}).

3.6. Distribution of $PM_{2.5}$ sources

$PM_{2.5}$ mass balance was assessed considering the following sources: secondary organic aerosol (OM_{SOA}), biomass burning (BB), fossil fuel

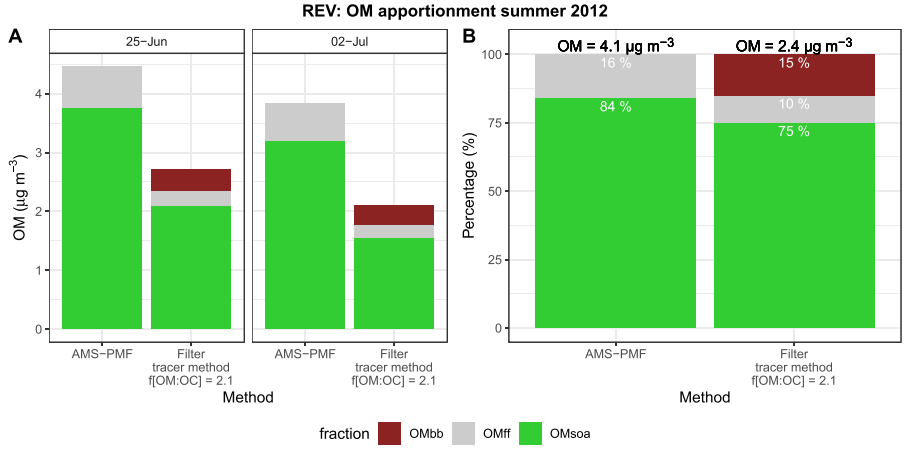

Fig. 3. Source apportionment of OM at REV for summer 2012 from AMS–PMF and from filter data.

(FF), nitrate, *nss*-sulphate, ammonium, dust and sea salt. Concentrations of BB were calculated as the sum of OM_{bb}, EC_{bb} and *nss-ndust*-K^+, and FF as the sum of OM_{ff} and EC_{ff}. SOA was the main $PM_{2.5}$ component at PEY (mean contribution of 44%), VER (38%) and REV (23%) (Fig. 4A). The SOA contribution at SND was 25% and 13% at OPE. Concentrations of primary anthropogenic emissions were similar at all sites with BB aerosols being 1.4–2.2 μg m^{-3} (17–27% of $PM_{2.5}$) and FF 0.3–0.5 μg m^{-3} (4–6% of $PM_{2.5}$), which altogether represented a quarter to a third of total $PM_{2.5}$ concentrations in 2012–2021. The range of BB contributions was similar to that at a French suburban site in 2013–2022 (~19%) (Jiao et al., 2023), at a peri–urban site in the North of France in 2016–2020 (Chebaicheb et al., 2023), and at rural sites in the UK in 2012–2020 (8 ± 20%) (Font et al., 2022). It is also similar to that at 15 urban sites in France (17 ± 9%) (Weber et al., 2019). Nitrate was the first (OPE) and second (REV) most abundant component of $PM_{2.5}$ with mean daily concentrations 2.4 and 1.7 μg m^{-3} (Table 1), representing 22% and 19% of $PM_{2.5}$, respectively. At the other sites, nitrate was in the range of 5.5–11% of $PM_{2.5}$ (Fig. 4A). At PEY, SND and VER, the third most abundant component was *nss*-SO_4^{2-} with mean daily concentrations of ~0.9 μg m^{-3}, which represented 12% of $PM_{2.5}$ at both PEY and VER and 17% at SND. Concentrations of *nss*-SO_4^{2-} were also noticeable at OPE and REV, with a mean concentration for the period of 1.4 μg m^{-3} (13% and 16% of total $PM_{2.5}$, respectively). Ammonium concentrations followed in terms of contribution with concentrations in the range 0.42–1.1 μg m^{-3} (Table 1). Ammonium contributed around 10% to $PM_{2.5}$ at REV and OPE; and 6–8% at PEY. Ionic balance between NH_4^+ *vs* the required to fully neutralize the measured sulphate and nitrate (in charge equivalents) was close to one at all sites (range: 0.83–1.03; median: 1.00) with little seasonal variability (not shown).

SIA represented the largest fraction of $PM_{2.5}$ at the OPE and REV, with contributions of roughly 45%. At the three other sites, the contribution was 22–31%. The largest contribution at OPE and REV can be explained by their geographical location, potentially more often downwind from NO_X and SO_2 hotspots such as Benelux, the UK and Western Germany (Fig. S17). In terms of contribution to $PM_{2.5}$, FF contributed less than 6% at all sites. Natural primary sources contributed marginally to $PM_{2.5}$: sea salt less than 2%; and mineral dust less than 4% except at OPE and SND that contributed 8–9% (Fig. 4A). Sea salt and dust aerosol particles are mostly found in the coarse fraction (Pérez et al., 2008; Putaud et al., 2010) and their contributions to $PM_{2.5}$ are therefore low. Overall, the comparison of the chemical composition at the five French rural background sites indicates the rural atmosphere in France is influenced by a quarter to a third by primary anthropogenic emissions (BB + FF = 22–33% of the total $PM_{2.5}$). However, the influence of secondary anthropogenic emissions (SIA) represents another quarter to a third at the central and southern sites while it increases up to almost a half in the northernmost sites. Assuming that OM_{SOA} is mostly of natural origin from the oxidation of volatile and semi-volatile organic compounds (Hallquist et al., 2009; Hodzic et al., 2016), natural sources (OM_{SOA} + dust + sea salt) represented 22–48% of the total $PM_{2.5}$ mass at the French rural background sites. However, some OM_{SOA} might originate from the oxidation of volatile and semi-volatile organic compounds of anthropogenic origin.

3.7. Seasonal and spatial variability of $PM_{2.5}$ sources

$PM_{2.5}$ monthly means calculated from those days with chemical composition data (Fig. 4B) and those calculated from the online $PM_{2.5}$ instrument (Fig. S8) were not statistically different as per the Wilcoxon signed–rank test. This validates the use of the $PM_{2.5}$ daily means for only

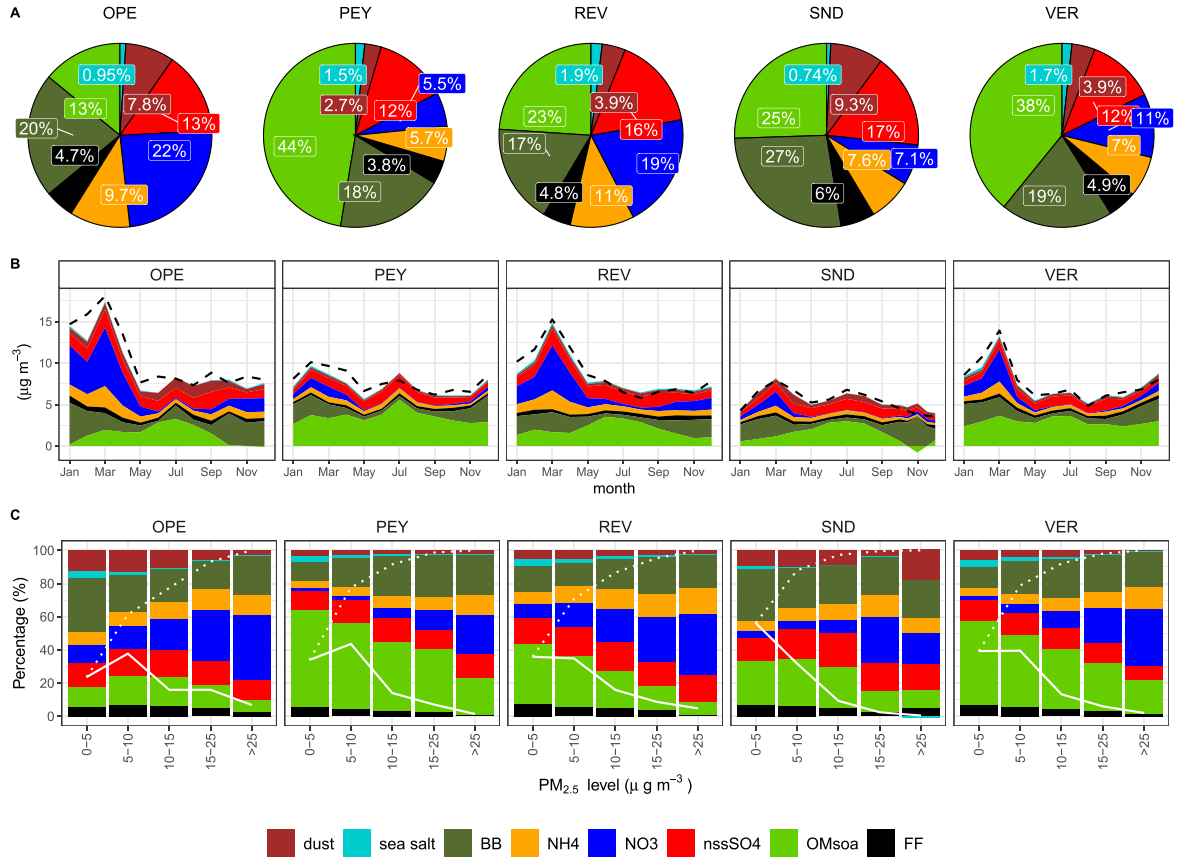

Fig. 4. $PM_{2.5}$ mass balance at the French rural sites. A) Average chemical composition of $PM_{2.5}$. B) Mean monthly $PM_{2.5}$ composition. Dashed line indicates the mean $PM_{2.5}$ from the collocated online instrument. C) Averaged chemical composition as a function of the $PM_{2.5}$ level. White solid line indicates the frequency for that given $PM_{2.5}$ level; dotted white line indicates the accumulated frequency.

those days with filter chemical composition to describe seasonal changes. $PM_{2.5}$ at the French rural sites were not homogenous neither in terms of aerosol levels nor their source distribution. First, the northernmost sites (OPE and REV) observed larger $PM_{2.5}$ concentrations (9–11 μg m^{-3} as long-term average 2012–2021) compared to the central (VER) and southern sites (PEY, SND), in the 6–7 μg m^{-3} range. The largest $PM_{2.5}$ concentrations were observed in March, with levels attaining approximately 15 μg m^{-3} at the northern sites of OPE and REV; and at the central site of VER. The peak in March was lower at the southern sites: 11 μg m^{-3} at PEY and 7 μg m^{-3} at SND. March concentrations were dominated by nitrate and ammonium at the northern sites (Fig. 4B). The larger contribution of ammonium nitrate in the north of France is in line with the prevalence of PM pollution episodes in the area (Chebaicheb et al., 2023; Favez et al., 2021; Roig Rodelas et al., 2019; Velazquez-Garcia et al., 2023). Sites in the north of France are closer to sources of aerosol precursors such as nitrogen oxides (NO_X) from highly populated areas in central and western Europe, and close to NH_3 hotspot in intensive agricultural areas such as the Netherlands and Belgium (Van Damme et al., 2015). In March, most European countries lift some of the winter restrictions for the application of manure to agricultural fields (Webb et al., 2013). This ammonia emissions combined with nitric acid, an oxidation product of NO_X, are the precursors of ammonium nitrate aerosols. Low boundary layer and cold temperatures in early spring promote the conversion of semi-volatile NH_4NO_3 from gas to particles (Seinfeld and Pandis, 2006). Conversely, such springtime episodes of SIA were less clear at the southernmost sites (PEY and SND) and the peak in March at the southern sites was mainly dominated by SOA and BB. PEY and SND also observed a second peak in July, of similar magnitude as that in March, but dominated by SOA (Fig. 4B). The lowest $PM_{2.5}$ concentrations were observed in August at OPE, REV and VER, with means of 7 μg m^{-3} (OPE and REV), and 5 μg m^{-3} (VER). The largest concentrations of *nss*-SO_4^{2-} occurred from June to October with levels around 1.5 μg m^{-3} at all sites (Fig. 4B). The enhanced photochemical activity in summer favours the oxidation of SO_2 and its conversion to sulphate (Salameh et al., 2015) in a period with larger shipping emissions especially in coastal cities (Gobbi et al., 2020). The oxidation of marine Dimethyl Sulfide (DMS) from phytoplankton might be also a source of sulphate at marine sites in summer (Pio et al., 2007). That was observed at VER in 2012–2014 and was related to air masses of marine origin (Golly et al., 2019). SND and REV observed a clear influence of *nss*–SO_4^{2-} in summer associated with air masses that had their origin on the sea: the Mediterranean Sea at SND; and the English Channel and the North Sea at REV. This was in agreement with enhanced maritime transport emissions expected at that time of year (Fig. S18).

3.8. Contribution of sources during pollution episodes

The contribution of each $PM_{2.5}$ source differed for those days with low daily $PM_{2.5}$ levels compared to those with larger $PM_{2.5}$ concentrations. Episodic days was defined based on the 2021 WHO daily guideline of 15 μg m^{-3} and those represented 23% of the days at OPE, 13% at REV, 8% at both PEY and VER, and less than 3% at SND (Fig. 4B). Episodic days (daily $PM_{2.5}$ > 15 μg m^{-3}) were enhanced in nitrate with contributions to $PM_{2.5}$ of ~30% at all sites except at PEY where the contribution was ~16%. The contribution of nitrate in non-exceeding days ($PM_{2.5}$ < 15 μg m^{-3}) was in the range of 4–15%. The enhancement in NO_3^- was also accompanied by an increase in the contribution of NH_4^+: from 6 to 10% in non–episodic days to 10–15% during episodes (Fig. 4C). Exceeding days were mostly associated with SIA, especially ammonium nitrate, in agreement with episodes on most mid-latitude and southern sites across Europe (Bressi et al., 2021).

BB also contributed at PEY on episodic days (27%) compared to non–episodic days (20%). SOA contributed largely to non–episodic days at all stations (25–45%) compared to episodic days (12–26%). Primary natural sources (dust and sea salt) also decreased their contribution on episodic days: from 2.8 to 6.3% (non–episodic); to 1–2.8% (episodic). SND was an exception to that trend with elevated contributions from dust on days with concentrations $PM_{2.5}$ > 25 μg m^{-3} with a mean contribution of 19% compared to contributions 4–10% for the rest of the days.

4. Conclusions

This paper presents the temporal and spatial distribution of $PM_{2.5}$ mass concentrations and its chemical composition at 5 rural background locations in France, that are most probably representative of a large fraction of the rural French territory and also some parts of Western Europe. Annual $PM_{2.5}$ in 2012–2021 ranged from 5 μg m^{-3} to 15 μg m^{-3}. Hence, only SND complied with the WHO annual guideline in 2019–2021; and REV in 2020. Exceedances of the daily WHO guideline were frequent especially from November to March. This suggests that the WHO targets for $PM_{2.5}$ concentrations might be difficult to attain in the short-term, even in the most rural parts of the territory.

A total of 2176 24-h samples covering 14% of the year were analysed for organic and elemental carbon and major inorganic ions. Mass balance of $PM_{2.5}$ was undertaken and representative ratios for biomass and fossil fuel emissions used to calculate the contribution of primary sources. SOA (18–35%) and SIA (22–45%) were the two main components of $PM_{2.5}$. The spatial distribution across mainland France highlighted a latitudinal gradient of SOA (greater at the southernmost sites) and SIA (larger at the northern sites). OC/EC ratios also observed a latitudinal increase towards the south during the summer maxima.

Biomass burning was the main primary source identified at the French rural background sites, with contributions 18–27% to $PM_{2.5}$ whereas FF contributed less than 6%. Episodes of $PM_{2.5}$ (daily $PM_{2.5}$ concentration >15 μg m^{-3} based on the daily 2021 WHO guideline) were significant at the northern sites (with a frequency of 13–23%), 8% at the centre and south-west of the country and weaker in the south-east (<3%). In the north, episodes were dominated by ammonium nitrate, while a combination of ammonium nitrate and biomass burning episodes is implicated in the south (PEY). Episodes in the south–east also observed increased contributions from dust.

Recently, online instruments with continuous monitoring of the chemical composition of fine PM (mainly in the PM_1 fraction) are available at multiple locations across Europe allowing for source apportionment of sources (Bressi et al., 2021; Chen et al., 2022). However, the reference method as per the EU directive is based on the filter method and then historic $PM_{2.5}$ datasets are mainly based on this off-line technique. There is a need to guarantee the consistency of the $PM_{2.5}$ source apportionment. Here, we compared the source apportionment undertaken on OM based on *nss-ndust*-K^+ for BB emissions and a representative OC/EC for FF. This was proved to report meaningful results, comparable with those obtained from online instrumentation.

Measurements of $PM_{2.5}$ and chemical composition at the rural background sites in France highlight that more effective policies are needed to reduce emissions of OM especially those associated with BB as well as ammonium nitrate concentrations, originated mostly from combustion (nitrate) and agricultural sources (ammonium). Overall, about half to three-quarters of the $PM_{2.5}$ mass at the French rural background sites are originated from anthropogenic emissions (either primary or secondary) indicating that further policies are needed to reduce ambient $PM_{2.5}$ levels.

CRediT authorship contribution statement

Anna Font: Writing – original draft, Visualization, Software, Methodology, Investigation, Formal analysis, Data curation, Conceptualization. **Joel F. de Brito:** Writing – review & editing, Methodology, Investigation, Conceptualization. **Véronique Riffault:** Writing – review & editing, Validation, Resources, Methodology, Investigation, Funding acquisition, Formal analysis, Data curation, Conceptualization. **Sébastien Conil:** Resources, Data curation. **Jean-Luc Jaffrezo:** Writing

– review & editing, Validation, Resources, Methodology, Investigation, Funding acquisition, Data curation, Conceptualization. **Aude Bourin:** Writing – review & editing, Resources, Project administration, Methodology, Investigation, Data curation.

Declaration of competing interest

The authors declare that they have no known competing financial interests or personal relationships that could have appeared to influence the work reported in this paper.

Data availability

Data will be made available on request.

Acknowledgments

This work was supported by the Ministry of Ecological Transition (MTE) and the French agency for ecological transition (ADEME). The authors would like to thank AirBreizh, Atmo Auvergne-Rhône-Alpes, Atmo Grand-Est, Atmo Occitanie and Lig'Air as well as Emmanuel Tison at IMT Nord Europe for their technical support in the field. Special thanks are given to Nicolas Bonnaire (Laboratoire des Sciences de l'Environnement et du Climat) for the laboratory analysis of ambient samples for the MERA sites; and Corentin Gouillou, Cécile Debevec and Benoît Herbin (IMT Nord Europe) for data validation of $PM_{2.5}$ mass concentration and chemical composition. The chemical analyses for the OPE data were performed at IGE on the analytical Air O Sol platform, with the work of many engineers. The authors gratefully acknowledge the NOAA Air Resources Laboratory (ARL) for the provision of the HYSPLIT transport and dispersion model used in this publication. IMT Nord Europe acknowledges financial support from the Labex CaPPA project, which is funded by the French National Research Agency (ANR) through the PIA (Programme d'Investissement d'Avenir) under contract ANR-11-LABX-0005-01, and the ECRIN project, both financed by the Regional Council "Hauts-de-France" and the European Regional Development Fund (ERDF).

Appendix A. Supplementary data

Supplementary data to this article can be found online at https://doi.org/10.1016/j.atmosenv.2024.120724.

References

Alastuey, A., Querol, X., Aas, W., Lucarelli, F., Pérez, N., Moreno, T., Cavalli, F., Areskoug, H., Balan, V., Catrambone, M., Ceburnis, D., Cerro, J.C., Conil, S., Gevorgyan, L., Hueglin, C., Imre, K., Jaffrezo, J.L., Leeson, S.R., Mihalopoulos, N., Mitosinkova, M., O'Dowd, C.D., Pey, J., Putaud, J.P., Riffault, V., Ripoll, A., Sciare, J., Sellegri, K., Spindler, G., Espen Yttri, K., 2016. Geochemistry of PM10 over Europe during the EMEP intensive measurement periods in summer 2012 and winter 2013. Atmos. Chem. Phys. 16, 6107–6129. https://doi.org/10.5194/acp-16-6107-2016.

Allen, A.G., Miguel, A.H., 1995. Biomass banting in the amazon: characterization of the ionic component of aerosols generated from flaming and smouldering rainforest and savannah. Environ. Sci. Technol. 29, 486–493. https://doi.org/10.1021/es00002a026.

Andreae, M.O., 1983. Soot carbon and excess fine potassium: long-range transport of combustion-derived aerosols. Science 220 (1979), 1148–1151. https://doi.org/10.1126/science.220.4602.1148.

Andreae, M., 2019. Emission of trace gases and aerosols from biomass burning– an updated assessment. Atmos. Chem. Phys. 19, 8523–8546.

Ball, A., Hill, R., Jenkinson, P., 2008. Integration of Air Quality Modelling and Monitoring Methods : Review and Applications.

Bhattarai, H., Saikawa, E., Wan, X., Zhu, H., Ram, K., Gao, S., Kang, S., Zhang, Q., Zhang, Y., Wu, G., Wang, X., Kawamura, K., Fu, P., Cong, Z., 2019. Levoglucosan as a tracer of biomass burning: recent progress and perspectives. Atmos. Res. 220, 20–33. https://doi.org/10.1016/j.atmosres.2019.01.004.

Borlaza, L.J., Weber, S., Marsal, A., Uzu, G., Jacob, V., Besombes, J.L., Chatain, M., Conil, S., Jaffrezo, J.L., 2022. Nine-year trends of PM10sources and oxidative potential in a rural background site in France. Atmos. Chem. Phys. 22, 8701–8723. https://doi.org/10.5194/acp-22-8701-2022.

Bressi, M., Cavalli, F., Putaud, J.P., Fröhlich, R., Petit, J.E., Aas, W., Äijälä, M., Alastuey, A., Allan, J.D., Aurela, M., Berico, M., Bougiatioti, A., Bukowiecki, N., Canonaco, F., Crenn, V., Dusanter, S., Ehn, M., Elsasser, M., Flentje, H., Prevot, A.S.H., 2021. A European aerosol phenomenology - 7: High-time resolution chemical characteristics of submicron particulate matter across Europe. Atmos. Environ. X (December 2020), 10. https://doi.org/10.1016/j.aeaoa.2021.100108.

Brito, J., Rizzo, L.V., Herckes, P., Vasconcellos, P.C., Caumo, S.E.S., Fornaro, A., Ynoue, R.Y., Artaxo, P., Andrade, M.F., 2013. Physical–chemical characterisation of the particulate matter inside two road tunnels in the São Paulo Metropolitan Area. Atmos. Chem. Phys. 13, 12199–12213. https://doi.org/10.5194/acp-13-12199-2013.

Calvo, A.I., Martins, V., Nunes, T., Duarte, M., Hillamo, R., Teinilä, K., Pont, V., Castro, A., Fraile, R., Tarelho, L., Alves, C., 2015. Residential wood combustion in two domestic devices: Relationship of different parameters throughout the combustion cycle. Atmos. Environ. 116, 72–82. https://doi.org/10.1016/j.atmosenv.2015.06.012.

Carslaw, D.C., Ropkins, K., 2012. Openair - an r package for air quality data analysis. Environ. Model. Software 27 (28), 52–61. https://doi.org/10.1016/j.envsoft.2011.09.008.

Caseiro, A., Bauer, H., Schmidl, C., Pio, C.a., Puxbaum, H., 2009. Wood burning impact on PM10 in three Austrian regions. Atmos. Environ. 43, 2186–2195. https://doi.org/10.1016/j.atmosenv.2009.01.012.

Chebaicheb, H., Brito, J.F. De, Chen, G., Tison, E., Favez, O., Marchand, C., Pr, S.H., 2023. Investigation of four-year chemical composition and organic aerosol sources of submicron particles at the ATOLL site in northern France. Environ. Pollut. 330, 121805 https://doi.org/10.1016/j.envpol.2023.121805.

Chen, G., Canonaco, F., Tobler, A., Aas, W., Alastuey, A., Allan, J., Atabakhsh, S., Aurela, M., Baltensperger, U., Bougiatioti, A., De Brito, J.F., Ceburnis, D., Chazeau, B., Chebaicheb, H., Daellenbach, K.R., Ehn, M., Haddad, I. El, Eleftheriadis, K., Favez, O., Flentje, H., Font, A., Fossum, K., Freney, E., Gini, M., Green, D.C., Heikkinen, L., Herrmann, H., Kalogridis, A.-C., Keernik, H., Lhotka, R., Lin, C., Lunder, C., Maasikmets, M., Manousakas, M.I., Marchand, N., Marin, C., Marmureanu, L., Mihalopoulos, N., Močnik, G., Nęcki, J., O'Dowd, C., Ovadnevaite, J., Peter, T., Petit, J.-E., Pikridas, M., Platt, S.M., Pokorná, P., Poulain, L., Priestman, M., Riffault, V., Rinaldi, M., Różański, K., Schwarz, J., Sciare, J., Simon, L., Skiba, A., Slowik, J.G., Sosedova, Y., Stavroulas, I., Styszko, K., Teinemaa, E., Timonen, H., Tremper, A., Vasilescu, J., Via, M., Vodička, P., Wiedensohler, A., Zografou, O., Minguillón, M.C., Prévôt, A.S.H., 2022. European aerosol phenomenology – 8: harmonised source apportionment of organic aerosol using 22 Year-long ACSM. AMS Datasets 166. https://doi.org/10.1016/j.envint.2022.107325.

Christiansen, A.E., Carlton, A.G., Porter, W.C., 2020. Changing nature of organic carbon over the United States. Environ. Sci. Technol. 54, 10524–10532. https://doi.org/10.1021/acs.est.0c02225.

Cordell, R.L., White, I.R., Monks, P.S., 2014. Validation of an assay for the determination of levoglucosan and associated monosaccharide anhydrides for the quantification of wood smoke in atmospheric aerosol. Anal. Bioanal. Chem. 406, 5283–5292. https://doi.org/10.1007/s00216-014-7962-x.

Cordell, R.L., Mazet, M., Dechoux, C., Hama, S.M.L., Staelens, J., Hofman, J., Stroobants, C., Roekens, E., Kos, G.P.A., Weijers, E.P., Frumau, K.F.A., Panteliadis, P., Delaunay, T., Wyche, K.P., Monks, P.S., 2016. Evaluation of biomass burning across North West Europe and its impact on air quality. Atmos. Environ. 141, 276–286. https://doi.org/10.1016/j.atmosenv.2016.06.065.

Crilley, L.R., Bloss, W.J., Yin, J., Beddows, D.C.S., Harrison, R.M., Allan, J.D., Young, D.E., Flynn, M., Williams, P., Zotter, P., Prevot, A.S.H., Heal, M.R., Barlow, J.F., Halios, C.H., Lee, J.D., Szidat, S., Mohr, C., 2015. Sources and contributions of wood smoke during winter in London: assessing local and regional influences. Atmos. Chem. Phys. 15, 3149–3171. https://doi.org/10.5194/acp-15-3149-2015.

Crippa, M., Decarlo, P.F., Slowik, J.G., Mohr, C., Heringa, M.F., Chirico, R., Poulain, L., Freutel, F., Sciare, J., Cozic, J., Di Marco, C.F., Elsasser, M., Nicolas, J.B., Marchand, N., Abidi, E., Wiedensohler, A., Drewnick, F., Schneider, J., Borrmann, S., Nemitz, E., Zimmermann, R., Jaffrezo, J.L., Prévôt, A.S.H., Baltensperger, U., 2013. Wintertime aerosol chemical composition and source apportionment of the organic fraction in the metropolitan area of Paris. Atmos. Chem. Phys. 13, 961–981. https://doi.org/10.5194/acp-13-961-2013.

EC, 2022. Proposal for a Directive of the European Parliament and the of the Council on ambient air quality and cleaner air for Europe [WWW Document]. URL. https://ec.europa.eu/info/law/better-regulation/have-your-say/initiatives/12677-Air-quality-revision-of-EU-rules_en.

El Haddad, I., Marchand, N., Dron, J., Temime-roussel, B., Quivet, E., Wortham, H., Luc, J., Baduel, C., Voisin, D., Luc, J., Gille, G., 2009. Comprehensive primary particulate organic characterization of vehicular exhaust emissions in France. Atmos. Environ. 43, 6190–6198. https://doi.org/10.1016/j.atmosenv.2009.09.001.

Favez, O., Weber, S., Petit, J.E., Alleman, L.Y., Albinet, A., Riffault, V., Chazeau, B., Amodeo, T., Salameh, D., Zhang, Y., Srivastava, D., Samaké, A., Aujay-Plouzeau, R., Papin, A., Bonnaire, N., Boullanger, C., Chatain, M., Chevrier, F., Detournay, A., Leoz-Garziandia, E., 2021. Overview of the French operational network for in situ observation of PM chemical composition and sources in urban environments (CARA program). Atmosphere 12 (2). https://doi.org/10.3390/atmos12020207.

Fine, P.M., Cass, G.R., Simoneit, B.R.T., 2002. Chemical characterization of fine particle emissions from the fireplace combustion of wood types grown in the midwestern and western United States. Environ. Eng. Sci. 21, 387–409. https://doi.org/10.1089/109287504323067021.

Font, A., Brito, J. F., Riffault, V., Conil, S., Jaffrezo J–L., Bourin, A. : Calculations of the Conversion Factor from Organic Carbon to Organic Matter for Aerosol Mass Balance – a Technical Note. Under Revision for *Atmospheric Pollution Research*.

Font, A., Ciupek, K., Butterfield, D., Fuller, G.W., 2022. Long-term trends in particulate matter from wood burning in the United Kingdom : dependence on weather and social factors. Environ. Pollut. 314, 120105 https://doi.org/10.1016/j.envpol.2022.120105.

Lai, C., Liu, Y., Ma, J., Ma, Q., He, H., 2014. Degradation kinetics of levoglucosan initiated by hydroxyl radical under different environmental conditions. Atmos. Environ. 91, 32–39. https://doi.org/10.1016/j.atmosenv.2014.03.054.

LCSQA, 2013. LCSQA, Métrologie des particules [WWW Document]. URL. http://www.lcsqa.org/rapport/2012/ineris/suivi-optimisation-utilisation-teom-fdms-bilan.

Gelencsér, A., May, B., Simpson, D., Sánchez-Ochoa, A., Kasper-Giebl, A., Puxbaum, H., Caseiro, A., Pio, C.A., Legrand, M., 2007. Source apportionment of PM2.5 organic aerosol over Europe: primary/secondary, natural/anthropogenic, and fossil/biogenic origin. J. Geophys. Res. Atmos. 112, 1–12. https://doi.org/10.1029/2006JD008094.

Gobbi, G.P., Di Liberto, L., Barnaba, F., 2020. Impact of port emissions on EU-regulated and non-regulated air quality indicators: the case of Civitavecchia (Italy). Sci. Total Environ. 719, 134984 https://doi.org/10.1016/j.scitotenv.2019.134984.

Golly, B., Waked, A., Weber, S., Samake, A., Jacob, V., Conil, S., Rangognio, J., Chrétien, E., Vagnot, M.P., Robic, P.Y., Besombes, J.L., Jaffrezo, J.L., 2019. Organic markers and OC source apportionment for seasonal variations of PM2.5 at 5 rural sites in France. Atmos. Environ. 198, 142–157. https://doi.org/10.1016/j.atmosenv.2018.10.027.

Hallquist, M., Wenger, J.C., Baltensperger, U., Rudich, Y., Simpson, D., Claeys, M., Dommen, J., Donahue, N.M., George, C., Goldstein, A.H., Hamilton, J.F., Herrmann, H., Hoffmann, T., Iinuma, Y., Jang, M., Jenkin, M.E., Jimenez, J.L., Kiendler-Scharr, A., Maenhaut, W., Mcfiggans, G., Mentel, T.F., Monod, A., Prévôt, A.S.H., Seinfeld, J.H., Surratt, J.D., Szmigielski, R., Wildt, J., 2009. The formation, properties and impact of secondary organic aerosol: current and emerging issues. Atmos. Chem. Phys. 9, 5155–5236.

Harrison, R.M., Beddows, D.C.S., Hu, L., Yin, J., 2012. Comparison of methods for evaluation of wood smoke and estimation of UK ambient concentrations. Atmos. Chem. Phys. 12, 8271–8283. https://doi.org/10.5194/acp-12-8271-2012.

He, L., Chen, H., Rangognio, J., Yahyaoui, A., Colin, P., Wang, J., Daële, V., Mellouki, A., 2018. Fine particles at a background site in Central France: chemical compositions, seasonal variations and pollution events. Sci. Total Environ. 612, 1159–1170. https://doi.org/10.1016/j.scitotenv.2017.08.273.

Hennigan, C.J., Sullivan, A.P., Collett, J.L., Robinson, A.L., 2010. Levoglucosan stability in biomass burning particles exposed to hydroxyl radicals. Geophys. Res. Lett. 37, L09806/1–L09806/4. https://doi.org/10.1029/2010GL043088.

Herich, H., Gianini, M.F.D., Piot, C., Močnik, G., Jaffrezo, J.L., Besombes, J.L., PrévÔt, A.S.H., Hueglin, C., 2014. Overview of the impact of wood burning emissions on carbonaceous aerosols and PM in large parts of the alpine region. Atmos. Environ. 89, 64–75. https://doi.org/10.1016/j.atmosenv.2014.02.008.

Hodzic, A., Kasibhatla, P.S., Jo, D.S., Cappa, C.D., Jimenez, J.L., Madronich, S., Park, R.J., 2016. Rethinking the global secondary organic aerosol (SOA) budget: stronger production, faster removal, shorter lifetime. Atmos. Chem. Phys. 16, 7917–7941. https://doi.org/10.5194/acp-16-7917-2016.

Hoffmann, D., Tilgner, A., Iinuma, Y., Herrmann, H., 2010. Atmospheric stability of levoglucosan: a detailed laboratory and modeling study. Environ. Sci. Technol. 44, 694–699. https://doi.org/10.1021/es902476f.

Hsu, S.C., Liu, S.C., Huang, Y.T., Chou, C.C.K., Lung, S.C.C., Liu, T.H., Tu, J.Y., Tsai, F., 2009. Long-range southeastward transport of Asian biosmoke pollution: signature detected by aerosol potassium in Northern Taiwan. J. Geophys. Res. Atmos. 114, 1–17. https://doi.org/10.1029/2009JD011725.

IPCC, 2021. Climate Change 2021: the Physical Science Basis. Contribution of Working Group I to the Sixth Assessment Report of the Intergovernmental Panel on Climate Change, vol. 3949. Cambridge University Press.

Jaffrezo, J.-L., Aymoz, G., Cozic, J., 2005. Size distribution of EC and OC in the aerosol of Alpine valleys during summer and winter. Atmos. Chem. Phys. 5, 2915–2925.

Jiao, Y., Ren, Y., Laroussi, W., Robin, C., Filippis, A. De, Bordier, F., 2023. Science of the Total Environment Tracking changes in atmospheric particulate matter at a semi-urban site in Central France over the past decade. Sci. Total Environ. 885, 163807 https://doi.org/10.1016/j.scitotenv.2023.163807.

Kaskaoutis, D., Kaskaoutis, D., Kaskaoutis, D., Grivas, G., Oikonomou, K., Tavernaraki, P., Papoutsidaki, K., Tsagkaraki, M., Stavroulas, I., Zarmpas, P., Paraskevopoulou, D., Bougiatioti, A., Liakakou, E., Gavrouzou, M., Dumka, U., Hatzianastassiou, N., Sciare, J., Gerasopoulos, E., Mihalopoulos, N., 2022. Environmental Pollution Impacts of severe residential wood burning on atmospheric processing , water-soluble organic aerosol and light absorption , in a medium-sized city of Southeastern Europe. Atmos. Environ. 280, 119139 https://doi.org/10.1016/j.atmosenv.2022.119139.

LCSQA, 2017. Vérification de la conformité technique des appareils de mesure pour la surveillance réglementaire de la qualité de l'air [WWW Document]. URL. https://imt-nord-europe.hal.science/hal-04250464.

Li, W., Ge, P., Chen, M., Tang, J., Cao, M., Cui, Y., Hu, K., Nie, D., 2021. Tracers from biomass burning emissions and identification of biomass burning. Atmosphere (Basel) 12. https://doi.org/10.3390/atmos12111401.

Lim, H.-J., Turpin, B.J., 2002. Origins of primary and secondary organic aerosol in Atlanta: results of time-resolved measurements during the Atlanta Supersite Experiment. Environ. Sci. Technol. 36, 4489–4496. https://doi.org/10.1021/es0206487.

Martinsson, J., Abdul Azeem, H., Sporre, M.K., Bergström, R., Ahlberg, E., Öström, E., Kristensson, A., Swietlicki, E., Eriksson Stenström, K., 2017. Carbonaceous aerosol source apportionment using the Aethalometer model-evaluation by radiocarbon and levoglucosan analysis at a rural background site in southern Sweden. Atmos. Chem. Phys. 17, 4265–4281. https://doi.org/10.5194/acp-17-4265-2017.

Mbengue, S., Fusek, M., Schwarz, J., Vodička, P., Šmejkalová, A.H., Holoubek, I., 2018. Four years of highly time resolved measurements of elemental and organic carbon at a rural background site in Central Europe. Atmos. Environ. 182, 335–346. https://doi.org/10.1016/j.atmosenv.2018.03.056.

Pérez, N., Pey, J., Querol, X., Alastuey, A., López, J.M., Viana, M., 2008. Partitioning of major and trace components in PM10-PM2.5-PM1 at an urban site in Southern Europe. Atmos. Environ. 42, 1677–1691. https://doi.org/10.1016/j.atmosenv.2007.11.034.

Petit, J.E., Favez, O., Sciare, J., Crenn, V., Sarda-Estève, R., Bonnaire, N., Močnik, G., Dupont, J.C., Haeffelin, M., Leoz-Garziandia, E., 2015. Two years of near real-time chemical composition of submicron aerosols in the region of Paris using an Aerosol Chemical Speciation Monitor (ACSM) and a multi-wavelength Aethalometer. Atmos. Chem. Phys. 15, 2985–3005. https://doi.org/10.5194/acp-15-2985-2015.

Pio, C.A., Legrand, M., Oliveira, T., Afonso, J., Santos, C., Caseiro, A., Fialho, P., Barata, F., Puxbaum, H., Sanchez-Ochoa, A., Kasper-Giebl, A., Gelencsér, A., Preunkert, S., Schock, M., 2007. Climatology of aerosol composition (organic versus inorganic) at nonurban sites on a west-east transect across Europe. J. Geophys. Res. Atmos. 112, 1–15. https://doi.org/10.1029/2006JD008038.

Pio, C., Cerqueira, M., Harrison, R.M., Nunes, T., Mirante, F., Alves, C., Oliveira, C., Sanchez de la Campa, A., Artíñano, B., Matos, M., 2011. OC/EC ratio observations in Europe: Re-thinking the approach for apportionment between primary and secondary organic carbon. Atmos. Environ. 45, 6121–6132. https://doi.org/10.1016/j.atmosenv.2011.08.045.

Putaud, J.-P., Raes, F., Van Dingenen, R., Brüggemann, E., Facchini, M.-C., Decesari, S., Fuzzi, S., Gehrig, R., Hüglin, C., Laj, P., Lorbeer, G., Maenhaut, W., Mihalopoulos, N., Müller, K., Querol, X., Rodriguez, S., Schneider, J., Spindler, G., Brink, H. Ten, Tørseth, K., Wiedensohler, A., 2004. A European aerosol phenomenology—2: chemical characteristics of particulate matter at kerbside, urban, rural and background sites in Europe. Atmos. Environ. 38, 2579–2595. https://doi.org/10.1016/j.atmosenv.2004.01.041.

Putaud, J.-P., Van Dingenen, R., Alastuey, a., Bauer, H., Birmili, W., Cyrys, J., Flentje, H., Fuzzi, S., Gehrig, R., Hansson, H.C., Harrison, R.M., Herrmann, H., Hitzenberger, R., Hüglin, C., Jones, a.M., Kasper-Giebl, a., Kiss, G., Kousa, a., Kuhlbusch, T.a.J., Löschau, G., Maenhaut, W., Molnar, a., Moreno, T., Pekkanen, J., Perrino, C., Pitz, M., Puxbaum, H., Querol, X., Rodriguez, S., Salma, I., Schwarz, J., Smolik, J., Schneider, J., Spindler, G., ten Brink, H., Tursic, J., Viana, M., Wiedensohler, a., Raes, F., 2010. A European aerosol phenomenology – 3: physical and chemical characteristics of particulate matter from 60 rural, urban, and kerbside sites across Europe. Atmos. Environ. 44, 1308–1320. https://doi.org/10.1016/j.atmosenv.2009.12.011.

Querol, X., Alastuey, A., Viana, M., Moreno, T., Reche, C., Minguillón, M.C., Ripoll, A., Pandolfi, M., Amato, F., Karanasiou, A., Pérez, N., Pey, J., Cusack, M., Vázquez, R., Plana, F., Dall'Osto, M., De La Rosa, J., Sánchez De La Campa, A., Fernández-Camacho, R., Rodríguez, S., Pio, C., Alados-Arboledas, L., Titos, G., Artíñano, B., Salvador, P., García Dos Santos, S., Fernández Patier, R., 2013. Variability of carbonaceous aerosols in remote, rural, urban and industrial environments in Spain: implications for air quality policy. Atmos. Chem. Phys. 13, 6185–6206. https://doi.org/10.5194/acp-13-6185-2013.

Ram, K., Sarin, M.M., Tripathi, S.N., 2012. Temporal trends in atmospheric PM 2.5, PM 10, elemental carbon, organic carbon, water-soluble organic carbon, and optical properties: impact of biomass burning emissions in the Indo-Gangetic Plain. Environ. Sci. Technol. 46, 686–695. https://doi.org/10.1021/es202857w.

Reid, J.S., Eck, T.F., Christopher, S.A., Koppman, R., Dubovik, O., Eleuterio, D.P., Holben, B.N., Reid, E.A., Zhang, J., 2005. A review of biomass burning emissions part III: intensive optical properties of biomass burning particles. Atmos. Chem. Phys. 5, 827–849. https://doi.org/10.5194/acp-5-827-2005.

Roig Rodelas, R., Perdrix, E., Herbin, B., Riffault, V., 2019. Characterization and variability of inorganic aerosols and their gaseous precursors at a suburban site in northern France over one year (2015–2016). Atmos. Environ. 200, 142–157. https://doi.org/10.1016/j.atmosenv.2018.11.041.

Salameh, D., Detournay, A., Pey, J., Pérez, N., Liguori, F., Saraga, D., Bove, M.C., Brotto, P., Cassola, F., Massabò, D., Latella, A., Pillon, S., Formenton, G., Patti, S., Armengaud, A., Piga, D., Jaffrezo, J.L., Bartzis, J., Tolis, E., Prati, P., Querol, X., Wortham, H., Marchand, N., 2015. PM2.5 chemical composition in five European Mediterranean cities: a 1-year study. Atmos. Res. 155, 102–117. https://doi.org/10.1016/j.atmosres.2014.12.001.

Samaké, A., Jaffrezo, J.L., Favez, O., Weber, S., Jacob, V., Albinet, A., Riffault, V., Perdrix, E., Waked, A., Golly, B., Salameh, D., Chevrier, F., Miguel Oliveira, D., Bonnaire, N., Besombes, J.L., Martins, J.M.F., Conil, S., Guillaud, G., Mesbah, B., Rocq, B., Robic, P.Y., Hulin, A., Le Meur, S., Descheemaecker, M., Chretien, E., Marchand, N., Uzu, G., 2019. Polyols and glucose particulate species as tracers of primary biogenic organic aerosols at 28 French sites. Atmos. Chem. Phys. 19, 3357–3374. https://doi.org/10.5194/acp-19-3357-2019.

Seinfeld, J.H., Pandis, S.N., 2006. Atmospheric Chemistry and Physics. From Air Pollution to Climate Change, 2nd ed. John Wiley & Sons, Inc., Hoboken, New Jersey.

Stein, A.F., Draxler, R.R., Rolph, G.D., Stunder, B.J.B., Cohen, M.D., Ngan, F., 2015. Noaa's hysplit atmospheric transport and dispersion modeling system. Bull. Am. Meteorol. Soc. https://doi.org/10.1175/BAMS-D-14-00110.1.

Van Damme, M., Clarisse, L., Dammers, E., Liu, X., Nowak, J.B., Clerbaux, C., Flechard, C.R., Galy-Lacaux, C., Xu, W., Neuman, J.A., Tang, Y.S., Sutton, M.A., Erisman, J.W., Coheur, P.F., 2015. Towards validation of ammonia (NH3) measurements from the IASI satellite. Atmos. Meas. Tech. 8, 1575–1591. https://doi.org/10.5194/amt-8-1575-2015.

Velazquez-Garcia, A., Crumeyrolle, S., de Brito, J.F., Tison, E., Bourrianne, E., Chiapello, I., Riffault, V., 2023. Deriving composition-dependent aerosol absorption, scattering and extinction mass efficiencies from multi-annual high time resolution

observations in Northern France. Atmos. Environ. 298, 119613 https://doi.org/10.1016/j.atmosenv.2023.119613.

Waked, A., Bourin, A., Michoud, V., Perdrix, E., Alleman, L.Y., Sauvage, S., Delaunay, T., Vermeesch, S., Petit, J.E., Riffault, V., 2018. Investigation of the geographical origins of PM10 based on long, medium and short-range air mass back-trajectories impacting Northern France during the period 2009–2013. Atmos. Environ. 193, 143–152. https://doi.org/10.1016/j.atmosenv.2018.08.015.

Webb, J., Sørensen, P., Velthof, G., Amon, B., Pinto, M., Rodhe, L., Salomon, E., Hutchings, N., Burczyk, P., Reid, J., 2013. An assessment of the variation of manure nitrogen efficiency throughout Europe and an appraisal of means to increase manure-N efficiency. Adv. Agron. https://doi.org/10.1016/B978-0-12-407247-3.00007-X.

Weber, S., Salameh, D., Albinet, A., Alleman, L.Y., Waked, A., Besombes, J.L., Jacob, V., Guillaud, G., Meshbah, B., Rocq, B., Hulin, A., Dominik-Sègue, M., Chrétien, E., Jaffrezo, J.L., Favez, O., 2019. Comparison of PM10 sources profiles at 15 French sites using a harmonized constrained positive matrix factorization approach. Atmosphere (Basel) 10, 1–22. https://doi.org/10.3390/atmos10060310.

Xu, L., Suresh, S., Guo, H., Weber, R.J., Ng, N.L., 2015. Aerosol characterization over the southeastern United States using high-resolution aerosol mass spectrometry: spatial and seasonal variation of aerosol composition and sources with a focus on organic nitrates. Atmos. Chem. Phys. 15, 7307–7336. https://doi.org/10.5194/acp-15-7307-2015.

Yttri, K.E., Dye, C., Braathen, O. -a., Simpson, D., Steinnes, E., 2009. Carbonaceous aerosols in Norwegian urban areas. Atmos. Chem. Phys. 9, 2007–2020. https://doi.org/10.5194/acp-9-2007-2009.

Yttri, K.E., Canonaco, F., Eckhardt, S., Evangeliou, N., Fiebig, M., Gundersen, H., Hjellbrekke, A.G., Lund Myhre, C., Matthew Platt, S., Prevot, A.S.H., Simpson, D., Solberg, S., Surratt, J., Tørseth, K., Uggerud, H., Vadset, M., Wan, X., Aas, W., 2021. Trends, composition, and sources of carbonaceous aerosol at the Birkenes Observatory, northern Europe, 2001-2018. Atmos. Chem. Phys. 21, 7149–7170. https://doi.org/10.5194/acp-21-7149-2021.

Zielinska, B., Sagebiel, J., Mcdonald, J.D., Whitney, K., Lawson, D.R., Zielinska, B., Sagebiel, J., Mcdonald, J.D., Whitney, K., Zielinska, B., Sagebiel, J., Mcdonald, J.D., Lawson, D.R., 2004. Emission rates and comparative chemical composition from selected in-use diesel and gasoline-fueled vehicles emission rates and comparative chemical composition from selected in-use diesel and gasoline-fueled vehicles. J. Air Waste Manage. Assoc. 54, 1138–1150. https://doi.org/10.1080/10473289.2004.10470973.